CFD MODELING AND CONSEQUENCE ANALYSIS OF AN ACCIDENTAL HYDROGEN RELEASE IN A LARGE SCALE FACILITY

Bauwens, C.R., and Dorofeev, S.B.
FM Global, Research Division, 1151 Boston-Providence Turnpike, Norwood, 02062, USA,
carl.bauwens@fmglobal.com

ABSTRACT

In this study, the consequences of an accidental release of hydrogen within large scale, (> 15,000 m^3), facilities were modeled. To model the hydrogen release, an LES Navier-Stokes CFD solver, called fireFoam, was used to calculate the dispersion and mixing of hydrogen within a large scale facility. The performance of the CFD modeling technique was evaluated through a validation study using experimental results from a 1/6 scale hydrogen release from the literature and a grid sensitivity study. Using the model, a parametric study was performed varying release rates and enclosure sizes and examining the concentrations that develop. The hydrogen dispersion results were then used to calculate the corresponding pressure loads from hydrogen-air deflagrations in the facility.

1.0 INTRODUCTION

The increased use of hydrogen fuel cell powered forklifts within warehouses presents a new safety concern due to the potential of an accidental release of hydrogen followed by an explosion. In particular, a leak from a hydrogen dispensing station, used to refuel the forklifts inside the warehouse, or from the forklift's storage tank itself, could rapidly release large quantities of hydrogen. Accidental releases of hydrogen are of particular concern due to the wide flammability limits and high reactivity of the fuel. For this study, hydrogen releases from the dispensing station itself, which has the potential to release much larger quantities of hydrogen, are examined.

To properly assess the potential for damage from an accidental explosion following a hydrogen release, and how this potential damage varies with release rate, requires an accurate estimate for how the hydrogen mixes with air. In particular, it is important to determine the mass of released hydrogen that remains above its lower flammability limit (LFL). To track the release of hydrogen from a simulated hydrogen dispensing station, Computation Fluid Dynamics (CFD) is used to estimate the mixing of hydrogen and air. The CFD tool fireFoam [1], an open source Large Eddy Simulation (LES) transient flow solver developed internally by FM Global, was used to perform this study.

This study is composed of two sets of simulations. The first component is a validation study used to assess the applicability of the CFD model for simulating hydrogen releases, while the second set are simulated releases from a hydrogen dispensing unit in a full warehouse geometry.

2.0 CFD METHODOLOGY

In this study, the CFD modeling was performed using fireFoam [1], an LES solver of the Navier-Stokes equations developed using the OpenFOAM CFD package. Although the solver was developed to simulate fires, it has robust numerical schemes for tracking the dispersion and mixing of different species. For the study, the combustion, radiation and pyrolysis components of fireFoam were not used and the solver was only used to model the dispersion and mixing of hydrogen in air. In these simulations, only two species were tracked, pure hydrogen and air. For all of the cases studied, low release velocities were used such that the mixing was dominated by buoyancy rather than momentum, which is consistent with a worst case scenario release where the released hydrogen immediately impinges on a solid surface and loses most of its momentum.

A mesh study was performed for the 1/6 scale geometry to determine the minimum mesh resolution that could be used for the large scale warehouse configuration. This was necessary as the large scale warehouse is an order of magnitude larger than the smaller scale experimental results and coarse mesh resolutions are necessary to perform the full scale simulations in a reasonable time frame.

3.0 CFD VALIDATION STUDY

3.1 Dispersion of Hydrogen

The intermediate scale hydrogen dispersions experiments used as the validation case were performed for Sandia National Laboratories at a test facility operated by SRI International [2]. The tests were performed in a 1/6 scale warehouse with hydrogen releases from a scaled forklift unit in an empty warehouse geometry. For these tests, hydrogen concentration was measured at various locations in the enclosure during the release. In addition to release tests, tests with combustion were also performed where the released mixture was ignited approximately 3 seconds into the release. Although tests were performed with and without ventilation, in this study only the tests without ventilation were examined.

Figure 1 shows the geometry used in these tests and the locations of six H_2 sensors whose results were reported in the paper. In the tests where the mixture was ignited, overpressure was measured at the center of the enclosure. To simulate a release deep within the forklift unit, the H_2 was dispersed through a small chamber inside the simulated forklift that was filled with steel beads. These beads were used to create a uniform release across the entire square 0.13 m x 0.13 m outlet.

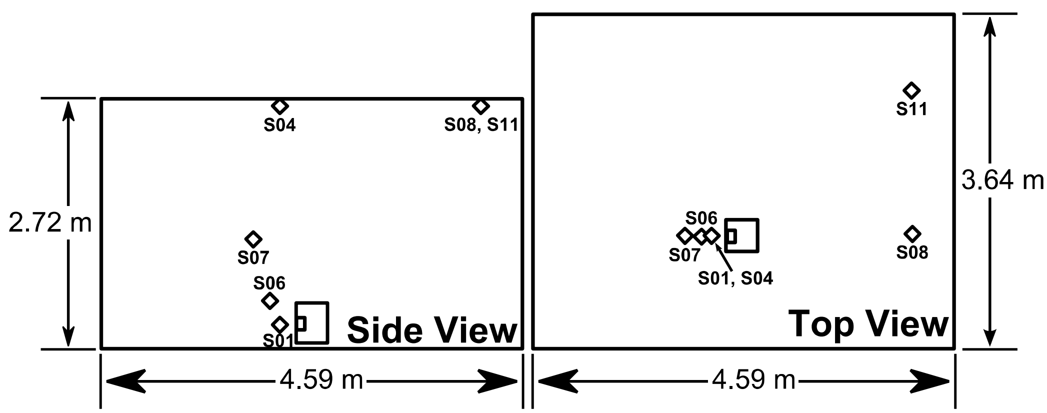

Figure 1. Illustration of dimensions of 1/6 scale warehouse and H_2 sensor locations

For each test, a hydrogen cylinder containing 0.0363 kg of hydrogen was used. The release from the cylinder was not regulated and the cylinder was simply blown down. To provide a release rate input for the CFD simulations, the release of the hydrogen had to be modeled. The release was modeled as an isentropic flow through an orifice, considering isentropic expansion of the hydrogen within the cylinder. Figure 2 compares the experimental release rate measurements with the input used for the simulation. Good agreement was found between the model and the experimental release rate.

For the small scale geometry, three mesh configurations were used representing different levels of grid refinement, identified as coarse, medium and fine. The coarse mesh had a uniform grid distribution with a resolution of 10cm. In order to accurately capture the size of the release area, however, local refinement was used in the vicinity of the release with a mesh resolution of 2.5 cm. The medium resolution mesh had local refinement of the mesh to 5 cm in all regions where the hydrogen was present and 2.5 cm resolution at the outlet. The fine resolution mesh had a resolution of 2.5 cm through the regions where hydrogen was present. Figure 3 shows the layout of the 1/6 scale geometry mesh with a cross section showing the local grid refinement present in the finest 2.5 cm mesh.

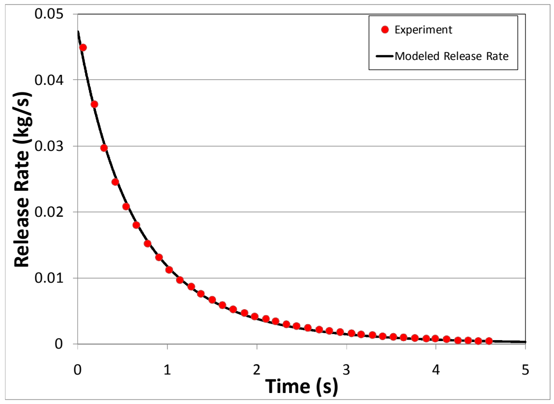

Figure 2. Comparison of experimental and modeled release rates for 1/6 scale warehouse

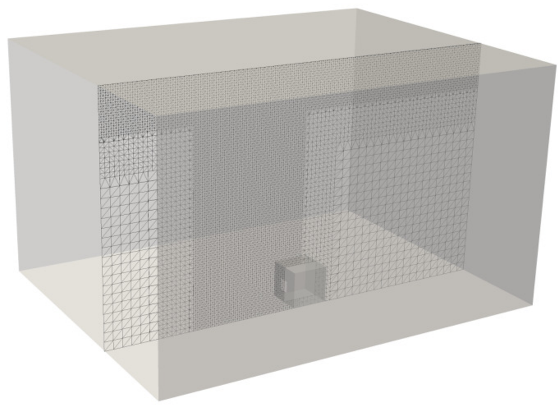

Figure 3. Illustration of mesh and refinement regions for 1/6 scale warehouse geometry

In figures 4-6 the hydrogen concentration measurements from two repeated experiments are compared with the simulation results for the three levels of mesh refinement. The results show that the simulations, in general, reproduced the experimental concentration measurements, particularly at later times. Differences that can be seen at location S06 where the concentration spike occurs earlier in simulations compared to the experiment. This difference is small, however, considering that this sensor is located far below the ceiling and a small change in the plume location would produce significant differences in the measurements recorded for this location.

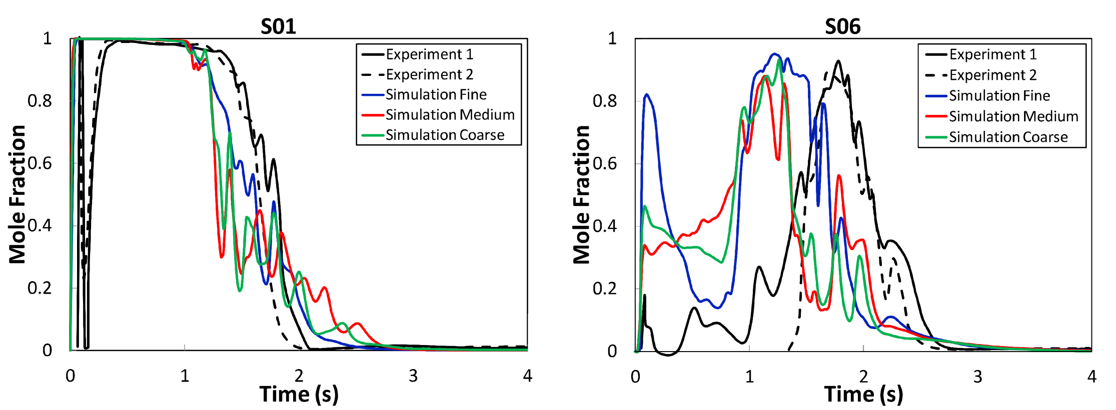

Figure 4. Comparison of experiment and simulation data for sensor locations S01 and S06

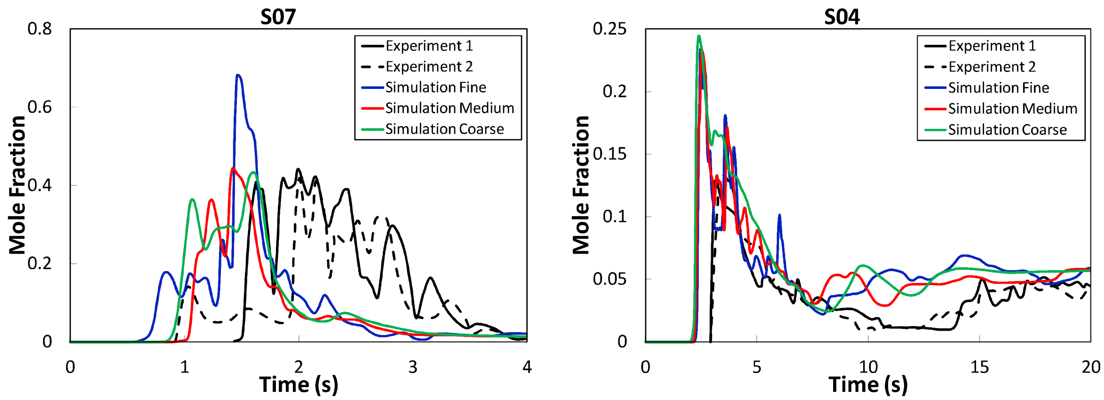

Figure 5. Comparison of experiment and simulation data for sensor locations S07 and S04

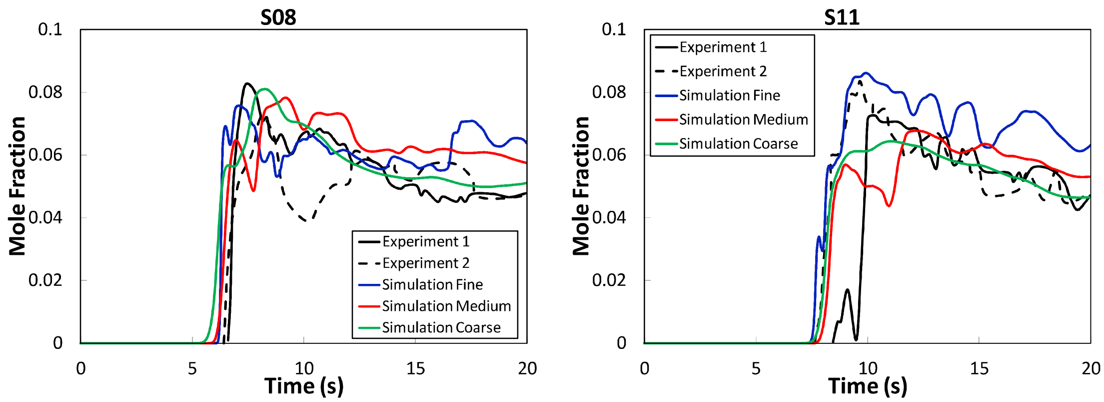

Figure 6. Comparison of experiment and simulation data for sensor locations S08 and S11

When the results are compared across different levels of grid refinement, the results are shown to be largely grid independent. There are slight variations in the results; however, these are likely caused by the natural variability of LES simulations.

The results of the simulations were also compared for how the total mass of hydrogen above the lower flammability limit (LFL), M_{LFL}, normalized by the total mass of hydrogen released, M_{Total}, varies with time for the different grid resolutions in Fig. 7. It is important to note that, in reality, the LFL of hydrogen varies depending on the direction of flame propagation, ranging from a concentration of 4% vol. when propagating upwards to 8% when propagating downwards [3]. For this study, a lower flammability limit of 6% was used to account for incomplete combustion at concentrations near the lower flammability limit. In general, the rate of mixing was consistent between the different mesh resolutions. The main difference is at low concentrations, after approximately 10 seconds, where the hydrogen in the coarsest mesh disperses faster. This effect is minimal, however, as this only happens after significant mixing occurs and the ceiling layer thickness is reduced to one to two computation cells.

These results show that the CFD approach used in this study reproduced the mixing at locations throughout the experimental enclosure. By reproducing the rate of mixing, the simulations also provide a good estimate for the quantity of hydrogen that remains in the flammable range after a release and can be used for the purpose of predicting the overpressure generated by combustion of the released hydrogen. The validation study also found that the 10 cm mesh provided a sufficient mesh resolution to ensure the results were relatively mesh independent.

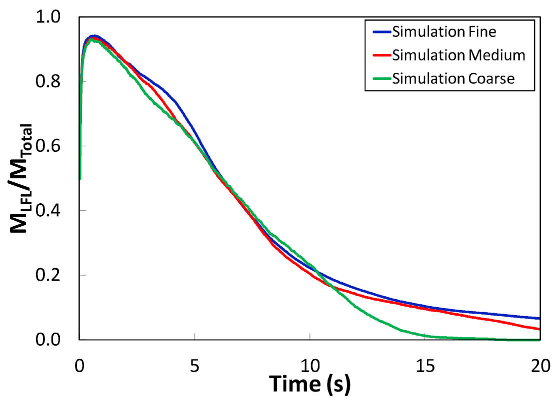

Figure 7. Comparison of mass above the LFL normalized by total mass released for different mesh resolutions

3.2 Overpressure

The Sandia experiments also included tests where the mixture was ignited approximately 3 s after the initial release the hydrogen. These experiments measured a maximum overpressure of 24.6 kPa when the mixtures was ignited near the forklift and a maximum overpressure of 18.9 kPa when the mixture was ignited at the ceiling. This difference illustrates the effect of the different LFLs of the mixture depending on the direction of flame propagation. When ignition takes place at the forklift, the flame propagates upwards and has a lower flammability limit of approximately 4%, consuming more of the hydrogen, particularly in the hydrogen plume between the forklift and the ceiling, and resulting in higher overall pressures. When ignition takes place at the ceiling, the flame propagates horizontally, and would have an effective LFL greater than 4%.

Estimates of the maximum pressure, caused by expansion of the burned gas and pressurization of the enclosure and not due to a blast wave, can be made assuming all of the hydrogen above the LFL is consumed. In addition to the pressurization analysis, blast damage distances will be provided for the full warehouse, large release, scenarios where blast wave generation is possible. Equation (1) describes how the adiabatic increase in pressure depends on the mass of hydrogen consumed:

$$\Delta p = p_0 \left[\left(\left(\frac{V_T + V_{H_2}}{V_T} \right) \left(\frac{V_T + V_{Stoich}(\sigma - 1)}{V_T} \right) \right)^{\gamma} - 1 \right] \tag{1}$$

where p_0 is the ambient pressure, V_T is the total volume of the warehouse, V_{H_2} is the expanded volume of pure hydrogen following the release, V_{Stoich} is the volume of a stoichiometric mixture of the consumed hydrogen, σ is the expansion ratio of a stoichiometric hydrogen-air mixture and γ is the specific heat ratio of air. The expanded volume is given by $V_{H_2} = M_{H_2} / \rho_{H_2}$ where M_{H_2} is the mass of hydrogen consumed and ρ_{H_2} is the density of hydrogen at ambient conditions and V_{Stoich} is V_{H_2} divided by the stoichiometric mole fraction of hydrogen.

Given a mass of hydrogen above the LFL at 3 s of 0.029 kg from the simulations, this approach produces an overall maximum overpressure of 24.4 kPa. This result is in close agreement with the experimental results when the mixture is ignited at the forklift, although it slightly over predicts the results when the mixture is ignited near the forklift. This result is expected, however, as ignition near the ceiling should not result in consumption of all of the fuel above the LFL, due to the downward propagation of the flame. This illustrates that the approach of using the total mass above the LFL produces results consistent with the experimental measurements.

4. WAREHOUSE CONFIGURATION RESULTS

The warehouse geometry used in this study had a cross section of 62.4 by 62.4 m and a height of 8 m. A total of 24 racks, 27.2 x1.2 m in cross section and 6.4 m in height were evenly distributed in the warehouse. The hydrogen dispenser was located along the wall of the warehouse 3.2 m from one of the corners. Figures 8, 9 and 10 show a top view, side view and isometric view of the enclosure respectively.

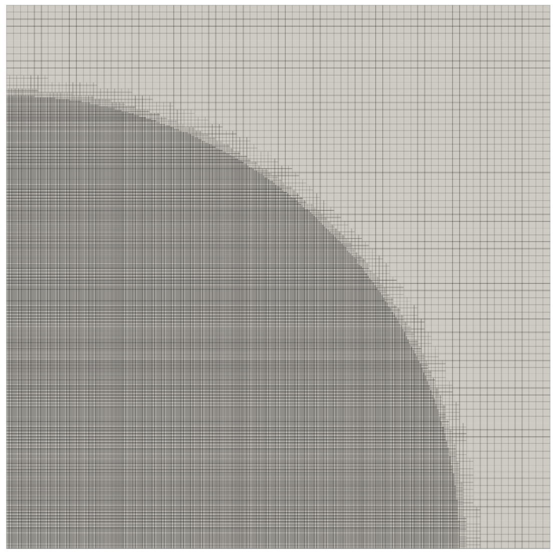

Figure 8. Top view of full scale warehouse mesh and refinement regions

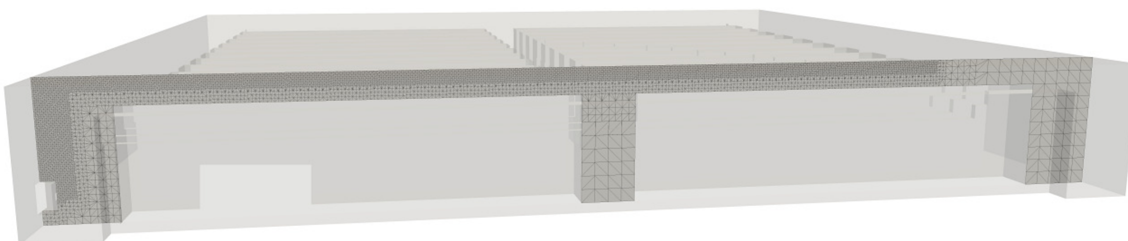

Figure 9. Side view of full scale warehouse mesh and refinement regions

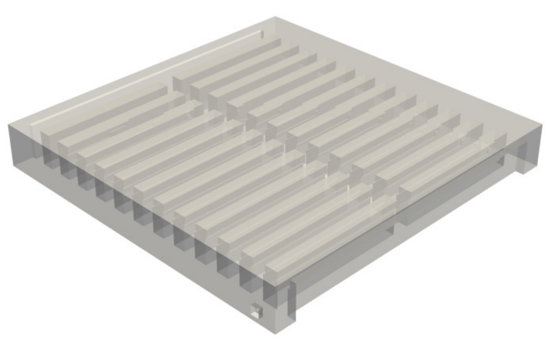

Figure 10. Isometric view of full scale warehouse mesh showing the locations of the racks and the hydrogen dispenser is shown at the corner of the warehouse located at the bottom of the image

The mesh generated for this geometry had an overall resolution of 0.8 m with local grid refinement. In the areas where hydrogen was present, the grid was refined to a resolution of 0.1 m. Due to the large scale of the warehouse, a finer mesh was not possible due to the prohibitive amount of time that would have required for simulations to be performed. A mesh resolution of 0.1 m, however, was shown to be sufficient to achieve grid independence in the smaller scale validation case.

For these simulations, a range of constant release rates were examined ranging from 0.25 kg/min up to 4 kg/min. To create a conservative estimate of the amount of released hydrogen in the flammable mixture, it was assumed that the hydrogen released from the dispenser hit a solid surface and was released with low momentum and rises as a buoyant plume. To provide a low momentum outlet for the dispenser, a large release area 0.24 m^2 was used. The simulations were run assuming a three minute release, at which time the final mass of hydrogen above the LFL was used to estimate the maximum overpressure.

Figures 11 and 12 below show example iso-contours of the LFL of the hydrogen release. For all of the release rates, the hydrogen cloud produces an expanding, symmetric, thin, circular cloud below the ceiling. The thickness of the cloud varied with the release rate but never approached the top of the racks. In the case of the 4 kg/min release, the cloud had an average thickness of approximately 0.45 m after three minutes.

Figure 11. Illustration of typical release show a side view iso-contour of LFL

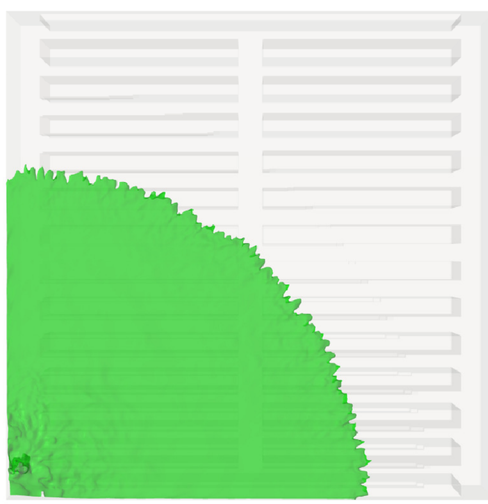

Figure 12. Illustration of typical release show a top view iso-contour of LFL

Figure 13 shows how the mass of hydrogen above the LFL varied with the release rate. It is interesting to note that, up to 2 kg/min, an increase in release rate results in proportionally less mixing and a larger fraction of the hydrogen above the LFL. When low mass flow rates were used, rates less than 1 kg/min, significant mixing occurs and negligible quantities of hydrogen remain above the LFL. At 2 kg/min and above, the rate of mixing between the hydrogen and air does not vary, and the fraction of hydrogen above the LFL appears to converge on the same curve, resulting in approximately

70% of the release hydrogen remaining in the cloud after the three minutes. To ensure that the increased mixing at lower release rates was accurately captured by the model, and not a product of the mesh resolution, a grid sensitivity study was performed for the 0.25 kg/min release. This study produced similar results for mesh resolutions up to 0.025 m, a resolution four times finer than was used for the simulations presented in Fig. 13.

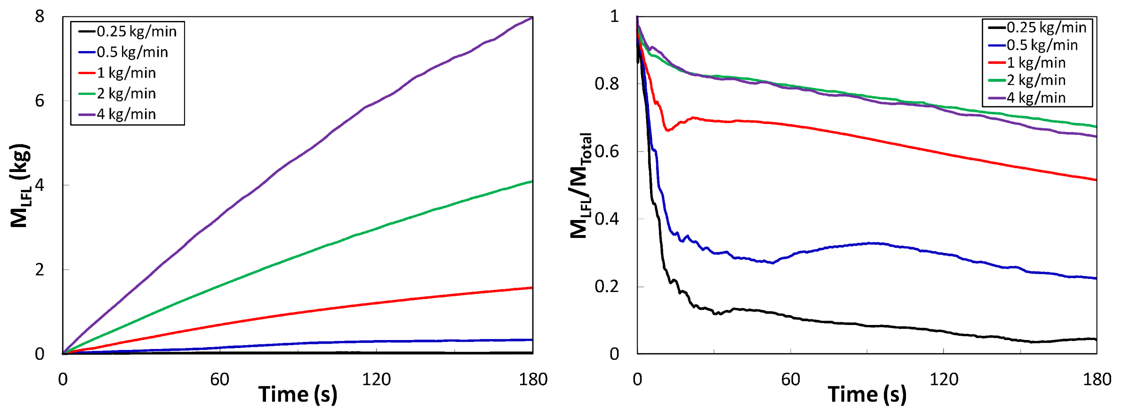

Figure 13. Summary of hydrogen mass above the lower flammability limit for the range of release rates.

For all of the releases, the main source of damaging overpressure was found to be the slow combustion of hydrogen that, without venting, results in a pressurization of the warehouse. In explosions, damage may also occur due to flame acceleration and the generation of a blast wave, however, for the releases seen in this study, the damage caused by the blast wave was minor. Table 1 below summarizing the results of the dispersion simulations as well as the overpressure estimates generated for the different release rates using Eq. (1). The overpressure results are shown for both the assumption that only the mass of hydrogen above the LFL is consumed (P_{max} above LFL) as well as if all of the hydrogen released is consumed (P_{max} Total). The volume taken by the racks themselves are included in the calculation for overpressure (reducing the total volume of the warehouse), however, they are assumed to only take up 60% of the overall rack volume. The results in Table 1 also assume that there is no ventilation and the enclosure is well sealed, without venting. In addition to the overpressure results, the table also includes estimates for the radius at which light damage may occur due to the generation of a blast wave using a previously developed technique for estimated damage from unconfined explosions [4]. These estimates are based on the mass of hydrogen above the LFL and represent the distance from the center of the cloud, located directly above the dispenser, where light damage could be expected. For the results presented in Table 1, the damage caused by the blast wave are small compared to the damage caused by the overall pressurization of the warehouse and would not cause any additional damage. If the warehouse was ventilated, however, and provided venting to a point where the peak internal pressures are significantly lower than 0.02 bar, then the contribution of the blast wave causing light damage within the specified radius may be the primary source of damage.

Table 1. Summary of Full Scale Unventilated Warehouse Simulation Results

Release Rate (kg/min)	M_{Total} (kg)	M_{LFL} (kg)	M_{LFL} (%)	P_{max} above LFL (bar)	P_{max} Total (bar)	Blast Wave Radius (m)
0.25	0.8	0.03	4.1%	-	0.01	-
0.5	1.5	0.34	22%	0.01	0.02	-
1	3.1	1.6	52%	0.02	0.04	5
2	6.1	4.1	67%	0.06	0.09	13
4	12.4	8.0	64%	0.12	0.18	23

5. DISCUSSION

5.1 Unventilated Warehouse

With overpressures at or below 0.02 bar, which may produce damage to windows and light damage to wall and roof panels [5, 6], significant damage would not be expected for release rates of 1 kg/min or lower. For a release rate higher than 1 kg/min, however, with overpressures above 0.02 bar, moderate damage to the enclosure would be likely. Above 0.1 bar, major damage to the enclosure could occur. For release rates in this region, or above, adequate protection for the enclosure would require a pressure relief system such as explosion vent panels or the addition of activate ventilation to the warehouse.

5.2 Ventilated Warehouse

The effect of ventilation was not examined explicitly in the CFD study for dispersion as the results are highly dependent on the location of the ventilation ducts and the ventilation rate. Commonly, the exhaust pick-ups of the ventilation system are located greater than 0.3 m below the ceiling of the warehouse. At this location, the ventilation ducts may not remove a significant quantity of hydrogen from the facility. If, however, the ventilation system is positioned in a location that would remove the hydrogen from the facility, such as directly above the dispenser or flush mounted at ceiling level, the expected overpressures within the warehouse could be reduced significantly. An additional consideration, however, is that a confined hydrogen explosion within the ventilation system could result in a far more severe explosion hazard due to flame acceleration if hydrogen concentration within the ventilation system exceed 10% vol. hydrogen [7, 8].

Concentration in the Ventilation System:

A simple conservative estimate for the maximum concentration in the ventilation system can be made by taking the ventilation rate of the enclosure, dividing it by the number of return vents, and assuming all of the hydrogen released enters a single vent. This can be expressed as:

$$C_{vent} = \frac{\dot{m}_{H_2}}{\rho_{H_2}} \frac{n}{\dot{V}_T} \tag{2}$$

where n is the number of vents and $\dot{V}_T$ is the total volumetric flow rate of the ventilations system.

For example, in the warehouse configuration used in this study, assuming three air changes per hour and eight return vents, the maximum concentration in the vent would be 12.4% for a 2 kg/min release and 24.8% for a 4 kg/min release. These results are conservative, and provides an upper bound as it assumes all of the hydrogen released goes into a single vent at the same rate it is released. In this case, the 2 kg/min case may not be a concern as the concentration is relatively close to the lower bound for possible flame acceleration; however, in the 4 kg/min case the concentration is high enough to present a significant flame acceleration hazard in the ducts. These results are not universal, however; with a different number of vents, ventilation rate or vent location the 2 kg/min case could also produce hazardous concentrations in the ventilation system.

Overpressure in the Ventilated Warehouse:

The ventilation rate can also be used to provide an estimate for the venting of the overpressure generated by the combustion of the hydrogen. The overpressures listed in Table 1 are for a completely sealed enclosure, however, in these releases the concentrations of hydrogen are particularly lean and the flame propagates slowly, releasing this pressure over a long period of time (on the order of a minute). Due to the slow rate of combustion, the amount of venting necessary to maintain minimal pressures may be close to the volumetric flow rate provided by the ventilation system.

The volumetric rate of gas production can be estimated if assumptions are made regarding the shape and concentration of the cloud. As seen in the Fig. 11 and 12, the released hydrogen takes the shape of a thin circular cloud. From the CFD simulations, the thickness and radius of these clouds up to the LFL concentration, were 0.35 m and 45.9 m respectively for the 2 kg/min release and 0.45 m and 54.4 m for the 4 kg/min release. If the cloud shape is assumed to be a quarter cylinder and concentration is approximated as uniform throughout the cloud, then an estimate for the concentration can be given by:

$$C_{cloud} = \frac{m_{H_2}}{\rho_{H_2} V_{cloud}} \tag{3}$$

where m_{H_2} is the mass of hydrogen above the LFL and V_{cloud} is the volume of the cloud. This calculation results in a cloud concentration of 8.6% for the 2 kg/min warehouse scenario and 9.2% for the 4 kg/min scenario.

In a flat layer the flame propagation velocity can be approximated as:

$$V_f = \sqrt{\sigma} S_L \tag{4}$$

where S_L is the laminar burning velocity of hydrogen at the concentration present in the cloud.

The maximum rate of volume generation due to combustion occurs when the flame reaches the edge of the cloud and is given by:

$$\dot{V}_{comb} = \frac{\pi h(\sigma - 1)\sqrt{\sigma} S_L R}{2} \tag{5}$$

where R is the radius of the cloud and h is the thickness of the cloud.

When $\dot{V}_{comb} < \dot{V}_T$ then the increase in pressure inside the warehouse due to combustion will be less than the pressure difference introduced by the ventilation system itself (although the total pressure rise would be the combination of the two). This is the case for both the 2 kg/min and 4 kg/min scenario outlined above if a ventilation rate of three air changes per hour is used.

The assumption that the cloud has a uniform concentration, however, may under predict the actual flame propagation speed and maximum flame area of a hydrogen flame in a cloud with varying concentration. To provide a more realistic estimate, the effective rate of energy release in the cloud should be increased to account for the effect of a non-uniform concentration. A reasonable estimate of the non-uniform concentration effect may be obtained by doubling the concentration in the cloud, with the cloud thickness reduced by a factor of two. In that case $\dot{V}_{comb} > \dot{V}_T$ for both the release rate of 2 kg/min and 4 kg/min. Assuming the chamber's ventilation system can accommodate explosion venting equivalent to the forced ventilation rate then the rise in pressure is given by the following equation:

$$\Delta p = p_0 \left[V_T^{-\gamma} \left(V_T + \frac{\pi h(\sigma - 1)}{4} R^2 - \frac{R \dot{V}_T}{\sqrt{\sigma} S_L} + \frac{\dot{V}_T^2}{\pi h(\sigma - 1)\sigma S_L^2} \right)^{\gamma} - 1 \right] \tag{6}$$

Recalculating the overpressures using equation (6) for the estimated non-uniform case, for three air changes per hour, gives an overpressure of 0.024 bar for the 2 kg/min case and 0.083 bar for the 4 kg/min case. Using the more realistic scenario the 2 kg/min case would produce light damage to the warehouse while the 4 kg/min case would still likely produce significant damage to the warehouse.

5.3 Other Warehouse Geometries

The results presented in this study are specific to the geometry of the warehouse modeled, however, for the same ceiling height, the rate of mixing would likely remain constant and the maximum pressure would simply scale with the volume as shown in Eq. (1) for unventilated warehouses and (6) for ventilated warehouses. If the ceiling height were increased, the mixing of the hydrogen with air would slightly increase and the percentage of fuel above the LFL would drop. Thus, a simple extrapolation to higher ceiling heights can be made by assuming the amount of hydrogen above the LFL remains constant.

Using these assumptions, Table 2 shows extrapolated peak overpressure results for warehouses with twice the footprint (7800 m^2), half the footprint (1950 m^2) of the base case as well as results for a higher 12.8 m ceilings (considering only the mass above the LFL). These results show the sensitivity of the overpressure peak to the volume of the enclosure. The ventilated cases are particularly sensitive to the volume of the warehouse, as the ventilation rate is determined by the volume. From these results it can be seen that for smaller warehouse geometries a release rate of 1 kg/min may still produce damaging overpressures in a ventilated warehouse. These results illustrate that importance of considering the overall volume of the warehouse when determining the maximum possible release rate for safe hydrogen dispensing.

Table 2. Peak Overpressures Extrapolated to Additional Warehouse Geometries

Height (m)	Area (m^2)	1 kg/min		2 kg/min		4 kg/min	
		Closed (bar)	Ventilated (bar)	Closed (bar)	Ventilated (bar)	Closed (bar)	Ventilated (bar)
8	1950	0.046	0.029	0.122	0.085	0.243	0.211
8	3900	0.023	0.007	0.061	0.024	0.119	0.083
8	7800	0.012	-	0.030	0.001	0.059	0.024
12.8	1950	0.029	0.012	0.076	0.038	0.150	0.114
12.8	3900	0.014	0.001	0.038	0.005	0.074	0.038
12.8	7800	0.007	-	0.019	-	0.037	0.006

<u>Additional Considerations</u>

The location of the dispenser would likely also have an effect on the rate of mixing between the hydrogen and air. However, based on observations that the lower release rate cases resulted in thinner hydrogen clouds and a faster rate of mixing it is reasonable to assume that if the release occurred away from the corner of the warehouse then the cloud would expand in more directions and result in a thinner cloud with more mixing, and a lower mass above the LFL. Thus the corner release provides the most conservative release location within the warehouse.

Also, the scenarios only considered a flat smooth ceiling for the warehouse. In reality, the ceiling of a typical warehouse would have a number of structural members as well as fixtures such as lights and sprinkler systems. These obstructions would cause increased mixing and further reduce the quantity of hydrogen above the LFL. However, if structural elements that restrict the spread of hydrogen along the ceiling are present, such as curtains or solid i-beam joists, the dispersion and mixing of the hydrogen would be reduced. In this scenario, higher concentrations of hydrogen would be achieved which could result in an accelerated flame and a blast wave causing damage to the warehouse.

6. CONCLUSION

CFD simulations of hydrogen releases were performed for two geometries, an intermediate scale representative warehouse geometry and in a full scale warehouse. The intermediate scale simulations were performed to provide a validation case for the CFD approach used in this study. Good agreement was found between the intermediate scale simulations and experimental data. These simulations found that mesh resolutions up to 10 cm were adequate to provide grid independent results for the dispersion simulations. Comparison with the experiments also showed that it is possible to produce a simple estimate of peak overpressure simply by considering the total mass of hydrogen above the lower flammability limit present in the enclosure.

The peak pressure that develops following ignition of a release of hydrogen within the warehouse was found to vary strongly with the release rate, volume of the warehouse and the presence of a ventilation system. For the specific warehouse geometry studied, without ventilation, a release rate of about 1 kg/min would result in light damage to the warehouse. Above 1 kg/min significant damage to the warehouse would be expected.

With a ventilation system, operating at a rate of three air changes per hour, and using conservative estimates for the cloud shape, it was found that, for a 31,200 m^3 warehouse, a release rate of about 2 kg/min would produce light damage to the warehouse while release rates above 2 kg/min would still produce significant damage to the warehouse. If a ventilation system is present, however, the system must be designed to prevent hydrogen concentrations within the ventilation system from exceeding 10%.

When the results of the study are extrapolated to smaller warehouse geometries, in this case a warehouse with half the footprint, even a 1 kg/min release may result in slight damage to a ventilated warehouse. These results imply that the overall volume of the warehouse must be considered when designing the maximum possible release rate of the system.

REFERENCES

1. Wang, Y., Chatterjee, P. and de Ris, J., Large eddy simulation of fire plumes, *Proc. Comb. Inst.*, **33**, No. 2, 2011, pp. 2473-2480.
2. Ekoto, I.W., Merilo, E.G., Houf, W.G., Evans, G.H. and Groethe, M.A., Experimental Investigation of Hydrogen Release and Ignition from Fuel Cell Powered Forklifts in Enclosed Spaces, 4th International Conference on Hydrogen Safety, Irvine, California, September, 2011.
3. Kumar, R.K., Flammability Limits of Hydrogen-Oxygen-Diluent Mixtures, *Journal of Fire Sciences*, **3**, No. 4, 1985, pp. 245-262.
4. Dorofeev, S.B., Evaluation of safety distances related to unconfined hydrogen explosions, *J. Hyd. Energy*, **32**, 2007, pp. 2118-2124.
5. Baker, W.E., Cox, P.A., Westine, P.S., Kulesz, J.J. and Strehlow, R.A., Explosion Hazards and Evaluation, 1983, Elsevier, Amsterdam, Oxford, New York.
6. Dorofeev, S. B., Kuznetsov, M.S., Alekseev, V.I., Efimenko, A.A., and Breitung, W., Evaluation of limits for effective flame acceleration in hydrogen mixtures, *Journal of Loss Prevention in the Processes Industries*, **14**, No. 6, 2001, pp 583-589.
7. Dorofeev, S.B. Flame acceleration and Explosion Safety Applications, *Proc. Comb. Inst.,* **33, 2011**, pp. 2161-2175.
8. National Fire Protection Association, The SFPE Handbook of Fire Protection Engineering, Third Edition, 2002, Society of Fire Protection Engineers, Bethesda, MD.